Global NEST Journal, Vol 26, No 2, 04606

Inhibition impact of major active ingredients of Jordanian *Peganum harmala* on the corrosion rate of Cu, Fe and Al metals

Ghassab M. Al-Mazaideh
Department of Pharmaceutical Chemistry, College of Pharmacy, University of Hafr Al Batin, P.O. Box 1803, Hafr Al-Batin 31991, Saudi Arabia
Received: 01/12/2022, Accepted: 26/01/2024, Available online: 29/01/2024
*to whom all correspondence should be addressed: e-mail: gmazaideh@uhb.edu.sa
https://doi.org/10.30955/gnj.004606

Graphical abstract

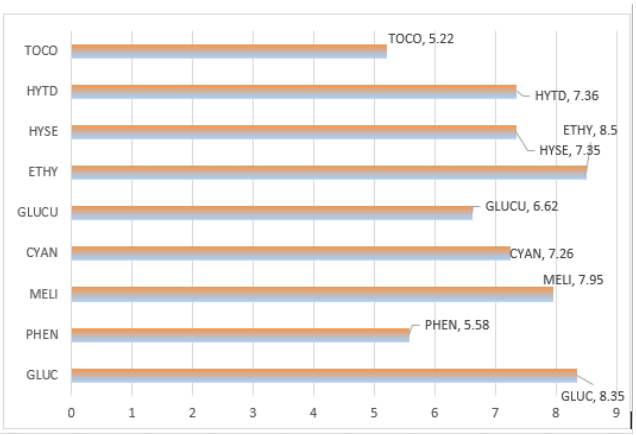

Abstract

The active components of Jordanian *Peganum harmala L.* (*P. harmala*) were investigated using both GC-MS and DFT calculations. The study focused on the methanol extract of *P. harmala* leaves, which was found to contain 21 significant natural components, of which 9 compounds constituted more than 2% of the total composition. These 9 compounds, including α-D-Glucopyranose (GLUC), Phenobarbital (PHEN), Melibiose (MELI), Cyanuric acid (CYAN), D-Glucuronic acid (GLUCU), Ethylamine (ETHY), 3-Hydroxysebacic acid (HYSE), 3-Hydroxytetradecanedioic acid (HYTD), and α-Tocopherol (TOCO), were evaluated as eco-friendly corrosion inhibitors for Al (Aluminium), Fe (Iron), and Cu (Cooper) metals using DFT calculations. The results showed that TOCO had the highest anti-corrosion performance among the 9 compounds, with Fe exhibiting the most inhibitory activity compared to Al and Cu. The high electrophilicity and Gibbs free energy of adsorbate value on metal surfaces made TOCO a distinguished corrosion inhibitor. The HOMO and LUMO gap of the inhibitors decreased in the following order: ETHY > GLUC > MELI > HYTD > HYSE > CYAN > GLUCU > PHEN > TOCO. These findings suggest that these chemicals may serve as environmental-friendly anticorrosion inhibitors for metal surfaces, although more in vitro experiments are needed to confirm these results.

Keywords: *Peganum harmala,* GC-MS, DFT, corrosion

1. Introduction

The cost of using corrosion inhibitors for active metals such as iron (Fe), copper (Cu), and aluminum (Al), as well as their reportedly serious side effects, have prompted researchers to look for other treatment methods for various metal corrosions that are environmentally friendly (G. M. Al-Mazaideh 2022; Amin, Ei-Rehim, El-Sherbini, Hazzazi, & Abbas 2009; F. Wedian, I. Mhaidat, N.A. Braik, & Al-Mazaideh 2022; I. Mhaidat, F. Wedian, Mifrig, & Al-Mazaideh, 2022). The inhibition procedure is attributed to the formation of a protective barrier on metals as a result of the inhibitor's adsorption. This layer prevents the active corrosion surface area from functioning, shielding the metal from further attack by the corrosive environment (Al-Itawi, Al-Mazaideh, Al-Rawajfeh, AMAMabreh, & Marashdeh, 2019; G. Al-Mazaideh, Ashram, & Khalyfeh, 2019; Sığırcık, Tüken, & Erbil, 2016). For instance, it has recently been discovered that a number of phytochemicals have potent anticorrosion efficacy, which can reduce the high rate of metal corrosion (Ikram, Jamil, & Fasehullah, 2022; Shaheen, & Ahmad, 2022; Nadeem Ahmad, Mirza, *et al.*, 2018). Phytochemicals offer a glimmer of hope for discovering new environmentally friendly inhibitors . Generally, natural substances have a wider range of chemical properties than synthetic ones, are more affordable to produce, and have negligible or no negative side effects

P. harmala is an Asian natural plant of the Nitrariaceae family that grows in the Middle East and areas of South Asia, especially in India and Pakistan (Sha'bani, Miraj, Rafieian-Kohpayei, & Namjoo, 2015). It is one of the most widely used folk medicinal plant species in Jordan (Ali-Shtayeh *et al.*, 2008; Khalid *et al.*, 2022).

P. harmala is a medical herb that is increasingly being utilized for psychotropic recreational purposes, such as in Ayahuasca analogs (Herraiz, González, Ancín-Azpilicueta, Arán, & Guillén, 2010). It was found that the extract of *P. harmala* possess scolicidal and bactericidal properties against many pathogenic bacteria due to their chemical composition (Al Qaisi *et al.*, 2022; Alani, Alqudah, & Tarawneh, 2021). These effects are attributed to the toxic effects of P. harmala, which are attributed to the major β-

carboline alkaloids harmine, harmalol, harmaline, and tetrahydroharmine . The alkaloids were found to be most abundant in the seeds and roots, least abundant in the stems and leaves, and absent in the blossoms (Herraiz *et al*., 2010).

Quantum chemical methods are important for explaining the absorptive behavior in addition to the mechanism of inhibitory action of various potential organic compounds (G. M. Al-Mazaideh, 2017; G. M. Al-Mazaideh, Ababneh, *et al*., 2016; G. M. Al-Mazaideh, Abu-Sbeih, & Khalil, 2017; G. M. Al-Mazaideh & Al-Quran, 2018; G. M. Al-Mazaideh, Al-Zereini, Al-Mustafa, & Khalil, 2016; Khalil, Al-Mazaideh, & Ali, 2016; Fadel Wedian, Al-Qudah, & Al-Mazaideh, 2017). This study aims to analyze the phytochemical composition of *P. harmala* using GC-MS analysis and to investigate the mechanism responsible for its anticorrosion activity . Quantum chemical techniques are being used for the first time to assess the protection efficiency of major phytonutrients in a methanolic extract of *P. harmala* as a new green organic inhibitor for Fe, Cu, and Al.

2. Materials and methods

2.1. Collection of plant materials

At the start of the 2021-spring term, Jordanian *P. harmala* plant wild-growing leaves were obtained from the Karak governorate. Al-Eisawi described the process of obtaining these leaves (Al-Eisawi, 1998). The plant's leaves have been drying in the shade, and isolated to be a consistent weight at room temperature, crushed, and saved in a dark place.

2.2. Extraction section

One gram of Jordanian *P. harmala* leaves was extracted in 10 ml of methanol and by constant stirring at room temperature for 4 days. For 10 minutes, the supernatant was then centrifuged at 4500 rpm. Next, the supernatant (3.0 ml) was moved to a 10 ml test tube and evaporated at room temperature. Before being injected into the GC-MS, the residues were reconstituted in 100 µL of BSTFA solution (N,O-bis (trimethylsilyl) trifluoroacetamide).

2.3. GC-MS analysis

The GC-MS analysis was carried out on an Agilent technology with model 6890 GC equipped by a Split-splitless injector and an HP-5MS capillary column coated with a 5 percent phenylmethylpolysiloxane film (30 m x 0.25 mm, 0.25 µm film thickness). The 6890 GC was outfitted with a 5973C mass spectrometer equipped with Inert MSD (Mass Spectrometer with mass Selective Detector and GC-MS). The column oven's temperature was programmed as follows: the temperature began at 60 °C and was gradually increased to 300°C with a ramp of 15 °C/min until remaining at 300 °C for 7 minutes before all elution was completed.

2.4. Computational details

A hybrid function called B3LYP with the basis set 6-31G*(d,p) was used to perform DFT calculations. Gaussian 09 (G09) was employed with the DFT-B3LYP method to optimize the molecules (Frisch, 2003). The calculated quantum parameters included Highest Occupied Molecular Orbitals (E_{HOMO}), Lowest Unoccupied Molecular Orbitals (E_{LUMO}), ΔE_{gap}, chemical potential (η), global softness (s), absolute hardness (X), fraction of transferred electrons (ΔN), and electrophilicity index (ω).

3. Results and discussion

3.1. GC-MS analysis of P. harmala extract

The phytoconstituents of *P. harmala* are visible in the GC-MS chromatogram (Figure 1), which has 21 peaks with retention durations ranging from 5.560 to 24.678 min. Each component was assessed and identified using mass fragmentation trends, by comparing them to benchmarks like Wiley 9 library spectral data as well as NIST standards.

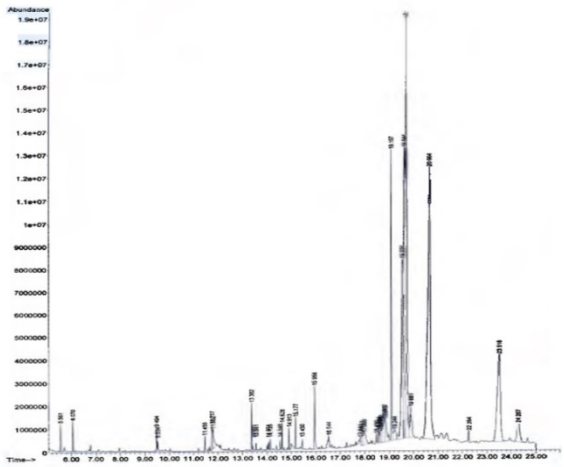

Figure 1. GC-MS chromatogram of the methanolic extract of P. harmala (RT = 5.56 - 24.678)

According to the study, the extract is made up of aromatic chemicals, carboxylic acids, saturated and unsaturated fatty acids, and oxygenated hydrocarbons. Table 1 displays the specific data of the 21 detected peaks. The methanolic extract of *P. harmala* included 9 primary recognized components with a composition area percent more than 2%. The major phytoconstituents present in the extract include **GLUC** (27.29%), **PHEN** (17.60%), **MELI** (10.56%), **CYAN** (6.62%), **GLUCU** (4.13%), **ETHY** (3.41%), **HYSE** (2.82%), **HYTD** (2.72%), and **TOCO** (2.62%) (Figure 2).

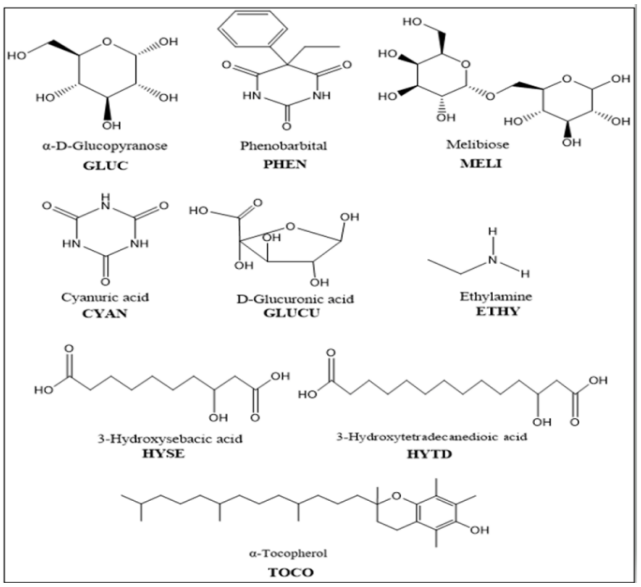

Figure 2. Major nine phytoconstituents of the methanolic extract of P. harmala

Table 1. GC-MS Results of detected phytochemicals of the P. harmala

NO.	Components	Retention Time (min)	Composition Percentage (%)
1.	Ethylamine	5.560	3.41
2.	Cyanuric acid	6.070	6.62
3.	1,3- Propanediol	9.493	1.93
4.	Androstan-3-one	11.455	0.02
5.	Malic acid	11.454	1.73
6.	N-Butylglycine	13.381	0.04
7.	Glucuronide	14.007	0.40
8.	L-Ascorbic acid	14.135	0.54
9.	3-Hydroxytetradecanedioic acid	14.629	2.72
10.	3-Hydroxysebacic acid	14.629	2.82
11.	Undecendioic Acid	14.912	1.81
12.	Palmitic acid	15.452	0.82
13.	D-Glucuronic acid	15.955	4.13
14.	Silane	16.264	0.37
15.	Isobutyric acid	16.544	1.41
16.	Hexadecanoic acid	18.583	0.85
17.	Phenobarbital	19.105	17.60
18.	α-D-Glucopyranose	19.108	27.29
19.	Melibiose	20.663	10.56
20.	α-Tocopherol	22.266	2.62
21.	β-Sitosterol	24.678	0.36

Table 2. Quantum descriptions for major phytoconstituents of a *P. harmala* using DFT (X_{Al} = 3.209, η_{Al} = 2.776, X_{Fe} = 4.026, η_{Fe} = 3.875, X_{Cu} = 4.480, η_{Cu} = 3.250) (F. Wedian, Mifrig, & Al-Mazaideh, 2022)

TOCO	HYTD	HYSE	ETHY	GLUCU	CYAN	MELI	PHEN	GLUC	Parameters
-4.97	-7.26	-7.31	-6.23	-7.20	-7.79	-6.72	-6.89	-6.85	E_{HOMO} (eV)
0.25	0.10	0.04	2.27	-0.58	-0.53	1.23	-1.31	1.50	E_{LUMO} (eV)
5.22	7.36	7.35	8.50	6.62	7.26	7.95	5.58	8.35	ΔE_{gap} (eV)
2.36	3.58	3.64	1.98	3.89	4.16	2.75	4.10	2.68	X
2.61	3.68	3.68	4.25	3.31	3.63	3.98	2.79	4.18	η
0.38	0.27	0.27	0.24	0.30	0.28	0.25	0.36	0.24	σ
0.08	0.03	0.03	0.08	0.06	0.07	0.03	0.08	0.04	ΔN_{Al}
0.13	0.03	0.03	0.12	0.01	0.01	0.08	0.01	0.08	ΔN_{Fe}
0.18	0.06	0.06	0.17	0.05	0.02	0.12	0.03	0.12	ΔN_{Cu}
1.98	1.40	1.40	1.21	1.56	1.42	1.30	1.85	1.23	ω_{Al}
3.11	2.20	2.21	1.91	2.45	2.23	2.04	2.90	1.94	ω_{Fe}
1.97	2.73	2.73	2.36	3.03	2.76	2.52	3.60	2.40	ω_{Cu}
2.37	2.28	1.72	1.39	3.98	0.01	0.95	1.17	2.38	μ (Debye)

3.2. Quantum chemical calculations

The adsorption efficiency of compounds over metallic surface and their chemical response are described by the Frontier Molecular Orbital Theory (FMO), which primarily reflects the relationship among molecular orbitals at E_{HOMO} and E_{LUMO} levels (I. Mhaidat *et al*., 2022). Computational DFT calculations have been performed for the nine major phytoconstituents of a *P. harmala*. The results of E_{HOMO} and E_{LUMO} molecular orbitals among these compounds are displayed in Table 2. A chemical reactivity toward metal surface adsorption is shown by the E_{HOMO}-E_{LUMO} gap, an alternative to ΔE_{gap} reflects the chemical reactivity of a molecule with metal surface adsorption is shown by the E_{HOMO}-E_{LUMO} gap, an alternative to the ΔE_{gap}. The inhibition efficiency increases as the forming complex stability between the organic chemical and the surface is raised, and the response of the molecule increases as the ΔE_{gap} decreases (Salman *et al*., 2021). Additionally, ΔE_{gap} defines the terms global hardening versus softness. A soft molecule also comes in a smaller form that is more reactive and facilitates easier polarity (Li, Deng, Fu, & Li, 2009). The molecule's polarizability is strongly associated with the term "global softness". To determine the impact of the nine main phytoconstituents of a *P. harmala* on the green corrosion inhibitory properties for Cu, Fe, and Al metals, the following global quantum chemical and molecular dynamic variables were calculated: ΔE_{gap}, E_{HOMO}, E_{LUMO}, σ, η, X, ΔN and ω.

According to Table 2, the ΔE_{gap} values of the nine inhibitors decrease in the following order: ETHY > GLUC > MELI > HYTD > HYSE > CYAN > GLUCU > PHEN > TOCO. As a result, TOCO, which has the minimum ΔE_{gap} (Figure 3) and σ among all compounds, is predicted to have strong inhibitor efficiency. This finding is supported by the inhibitor's σ

calculation, and Table 3 shows its reactivity and additionally, it is evident that TOCO has the lowest values for η across the board for all compounds. This observation is a reflection of the impact of σ, as a soft molecule is more responsive than a hard one, and the maximum σ and lowest η values of TOCO designate it as the best inhibitor (Awad, Mustafa, & Elnga, 2010). Compared to the other inhibitors, the ΔN analysis indicates that the TOCO molecule is the predominant source of electrons transferred to the surfaces of the metals (Al, Fe, and Cu). The inhibitor's ability to accept electrons from metals is indicated by the ω.

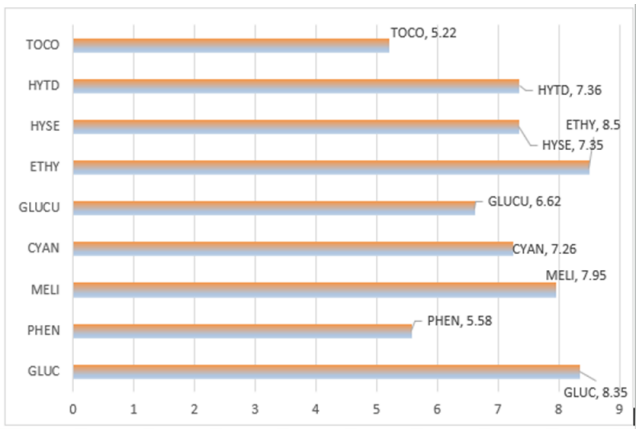

Figure 3. ΔEgap of the major nine phytoconstituents of the methanolic extract of P. harmala

Compared to the other inhibitors, TOCO has the highest ω values, and its impact on metals is as follows: Fe > Al > Cu. This conclusion is consistent with the experimental published research (F. Wedian, Mhaidat, Braik, & Al-Mazaideh, 2022). The electrochemical results revealed that TOCO has a quick adsorption process and generates a thick protective coating on the surface of Fe. The interaction between oxygen atoms with Fe sites produces the Fe-TOCO complex, which prevents oxide formation. As a result , this discovery verifies its strong capacity to receive electrons from metals. In other words, , metals operate as Lewis bases, whereas all chemicals act as Lewis acids (cathodic inhibitor). To form a coordinated bond , the metal will take electrons from the inhibitor. Furthermore, depending on the location of the optimal structure of such inhibitor on the space, the inhibitor can absorb electrons from metal to establish back-donating bonds. Donation and back-donation processes improve inhibitor adsorption on the metal surface, leading to an increase in inhibition effectiveness.

3.2.1. Inhibition mechanism

The nine inhibitors can adsorb , and hetero-atoms of oxygen, nitrogen, as well as π-electrons of aromatic rings are involved (Musa, Kadhum, Mohamad, Rahoma, & Mesmari, 2010). The findings imply that TOCO can bind to surfaces by electron donation from electron-rich centers to the open d-orbitals of the investigated metals in addition to accepting electrons from such surfaces of the metals, formulating a back-donating bond that is dependent on the orientation of its optimized inhibitor structure here on spatial plane.

The results indicate that TOCO has the highest ability to adsorb on metal surfaces because it can donate its unshared electron pairs from O atoms to the vacant d-orbitals of metals . In an acidic media, inhibitors can bind to metal surfaces through physisorption and chemisorption. The difference in chemical potentials between the metal and the inhibitor determines the extent of adsorption. With Al, Fe, and Cu, the computed ΔG_{ads} for TOCO are -81.92 kJ/mol, -160.12 kJ/mol, and -204.55 kJ/mol, respectively. Based on the ΔG_{ads} values ranging between -80 and -400 kJ/mol, TOCO is likely adsorbing through spontaneous chemical adsorption (F. Wedian, Mifrig, *et al*., 2022).

4. Conclusion

For the first time, the primary active phytonutrients of Jordanian *P. harmala* were investigated for their ability to control corrosion, and they were effectively used as green corrosion inhibitors on the surfaces of significant metals (Al, Fe, Cu). The effectiveness of inhibition was found to be influenced by the heteroatom content of the natural substances. The methanolic extracted of *P. harmala* leaves was studied for its anticorrosion ingredients, and assessed using a GC-Mass and DFT techniques on the main active green phytonutrients towards three metals. The extract has 21 primary natural components, according to the results of GC-MS. In nine of the 21 compounds, the composition percent is more than 2%. Theoretical models provided a clear picture of how various green inhibitors affected the rate of corrosion of metals. The theoretical findings showed that GLUC, PHEN, MELI, CYAN, GLUCU, ETHY, HYSE, and TOCO have good anticorrosion properties, with TOCO serving as the most effective and greenest inhibitor for all metals. TOCO has a small ΔE_{gap} and can interact strongly with metals (Al, Fe, and Cu), which makes it highly effective in inhibiting corrosion . It also demonstrated impressive inhibition efficiency with Fe as an anodic inhibitor. Furthermore, this finding explained the experimental electrochemical measurements of the interaction between oxygen atoms from TOCO and metal sites, resulting in the formation of a TOCO–M (Al, Fe, Cu) complex that prevented oxide formation.

Acknowledgements

The author wishes to express his gratitude to the Deanship of Scientific Research at the University of Hafr Al Batin in Saudi Arabia for their unending support of this research.

Conflict of interest

The author has no conflicts of interest to declare that are relevant to the content of this article.

Availability of data and material

The author declares that there is no data that supports the findings of this study.

References

Ahmad M.N., Anjum M.N., Nawaz F., Iqbal S., Saif M.J., Hussain T., Mujahid A., Farooq M.U., Nadeem M., Rahman A., Raza (Late) A. and Shehzad K. (2018). Synthesis and antibacterial potential of hybrid nanocomposites based on

polyorthochloroaniline/copper nanofiller. *Polym. Compos.*, **39**, 4524-4531. https://doi.org/10.1002/pc.24558.

Al Qaisi Y.T., Khleifat K.M., Oran S.A., Al Tarawneh A.A., Qaralleh H., Al-Qaisi T.S. and Farah H.S. (2022). Ruta graveolens, Peganum harmala, and Citrullus colocynthis methanolic extracts have in vitro protoscolocidal effects and act against bacteria isolated from echinococcal hydatid cyst fluid. *Arch Microbiol,* **204**(4), 228. doi: 10.1007/s00203-022-02844-7.

Alani W.K., Alqudah A.A. and Tarawneh K A. (2021). Antibacterial and Antioxidant Activities of Ethanol Extracts of Some Plants Selected from South Jordan. *Pharmacogn Journal,* **13**(2), 528–534. doi: 10.5530/pj.2021.13.6.

Al-Eisawi D.M. (1998). *Field Guide to Wild Flowers of Jordan and Neighbouring Countries*: Jordan Press-Foundation "Al-Rai" , Amman.

Ali-Shtayeh M.S., Jamous R.M., Al-Shafie J.H., Elgharabah W.A., Kherfan F. A., Qarariah K.H., Nasrallah H.A. (2008). Traditional knowledge of wild edible plants used in Palestine (Northern West Bank): A comparative study. *Journal of Ethnobiology and Ethnomedicine,* **4**(1), 13. doi: 10.1186/1746-4269-4-13.

Al-Itawi H., Al-Mazaideh G., Al-Rawajfeh A., AMAMabreh and Marashdeh A. (2019). The effect of some green inhibitors on the corrosion rate of Cu, Fe and Al metals. *International journal of corrosion and inhibition scale,* **8**(2), 199–211. doi: 10.17675/2305-6894-2019-8-2-3

Al-Mazaideh G., Ashram M. and Khalyfeh K.A. (2019). Corrosion and Electrochemical Studies on the Stability of New Thiacrown Ethers Derived from Quinoline. *Jordan Journal of Chemistry,* **14**(3), 89–96.

Al-Mazaideh G.M. (2017). Carbohydrates as Green Corrosion Inhibitors of Copper: Ab initio Study. *Jordan Journal of Chemistry,* **12**(4), 189–200.

Al-Mazaideh G.M. (2022). Monosaccharides as green corrosion inhibitors of iron (Fe) and aluminium (Al) metals *International Journal of Corrosion and Scale Inhibition,* **11**(1), 280–292. doi: 10.17675/2305-6894-2022-11-1-16.

Al-Mazaideh G.M. and Al-Quran S.A. (2018). Inhibitive action of Chamomile extract on the corrosion of Iron: Density Functional Theory. *Moroccan Journal of Chemistry,* **6**(1), 195–202. doi:https://doi.org/10.48317/IMIST.PRSM/ morjchem-v6i1.8883.

Al-Mazaideh G.M., Ababneh T.S., Abu-Shandi K.H., Jamhour R.M.A.Q., Salman H.J.A., Al-Msiedeen A.M. and Khalil S.M. (2016). DFT calculations of Mesembryanthemum nodiflorum compounds as corrosion inhibitors of aluminum. *Physical Science International Journal,* **12**(1), 1–7. doi: 10.9734/PSIJ/2016/28273.

Al-Mazaideh G.M., Abu-Sbeih K.A. and Khalil S.M. (2017). Computational Calculations of Chitosan Fragments as Corrosion Inhibitors of Metals. *Journal of Chemical, Biological and Physical Sciences,* **7**(2), 398–409.

Al-Mazaideh G.M., Al-Zereini W.A., Al-Mustafa A.H. and Khalil S.M. (2016). The effect of nitro maleimides from a marine vibrio species compounds as a source of environment-tally friendly corrosion inhibitors for metals: A computational Study. *Advances in Enviromental Bilogy,* **10**(8), 159–168.

Amin M.A., Ei-Rehim S.S.A., El-Sherbini E. E.F., Hazzazi O.A. and Abbas M.N. (2009). Polyacrylic acid as a corrosion inhibitor for aluminium in weakly alkaline solutions. Part I: Weight loss, polarization, impedance EFM and EDX studies. *Corrosion Science,* **51**(3), 658–667. doi: https://doi.org/10.1016/ j.corsci.2008.12.008.

Awad M.K., Mustafa M.R. and Elnga M.M. A. (2010). Computational simulation of the molecular structure of some triazoles as inhibitors for the corrosion of metal surface. *Journal of Molecular Structure: THEOCHEM,* **959**(1), 66–74. doi: https://doi.org/10.1016/j.theochem.2010.08.008.

Frisch M.J. *et al*. (2003). Gaussian, Inc., Wallingford, CT.

Herraiz T., González D., Ancín-Azpilicueta C., Arán V.J. and Guillén H. (2010). beta-Carboline alkaloids in Peganum harmala and inhibition of human monoamine oxidase (MAO). *Food Chem Toxicol,* **48**(3), 839–845. doi: S0278-6915(09)00601-2.

Ikram A., Jamil S. and Fasehullah M. (2022). Green synthesis of copper oxide nanoparticles from papaya/lemon tea extract and its application in degradation of methyl orange. *Mater. Materials Innovations*, *2*, 115–122.

Khalid M., Amayreh M., Sanduka S., Salah Z., Al-Rimawi F., Al-Mazaideh G. M., Shalayel M.H.F. (2022). Assessment of antioxidant, antimicrobial, and anticancer activities of Sisymbrium officinale plant extract. *Heliyon,* **8**, e10477. doi: https://doi.org/10.1016/j.heliyon.2022.e10477.

Khalil S.M., Al-Mazaideh G.M. and Ali N.M. (2016). DFT Calculations on Corrosion Inhibition of Aluminum by Some Carbohydrates. *International Journal of Biochemistry Research & Review,* **14**(2), 1–7. doi: 10.9734/IJBCRR/ 2016/29288.

Li X., Deng S., Fu H. and Li T. (2009). Adsorption and inhibition effect of 6-benzylaminopurine on cold rolled steel in 1.0M HCl. *Electrochimica Acta,* **54**(16), 4089–4098. doi: https://doi.org/10.1016/ j.electacta.2009.02.084.

Mhaidat I., Wedian F., Mifrig A.Z. and Al-Mazaideh G.M. (2022). Inhibition impact of synthesized mercapto- and alkylthio-triazole compounds on the corrosion of aluminum in acidic solution. *International Journal of Corrosion and Scale Inhibition,* **11**(3), 1083–1099. doi: 10.17675/2305-6894-2022-11-3-11.

Musa A.Y., Kadhum A.A.H., Mohamad A.B., Rahoma A.A.B. and Mesmari H. (2010). Electrochemical and quantum chemical calculations on 4,4-dimethyloxazolidine-2-thione as inhibitor for mild steel corrosion in hydrochloric acid. *Journal of Molecular Structure,* **969**(1), 233–237. doi: https://doi.org/10.1016/j.molstruc.2010.02.051.

Salman H.A., Yaakop A.S., Al-Mustafa A., Tarawneh K., Aladaileh S., Al-Rimawi F. and Wahab H. (2021). The dual impact of Jordanian Ephedra alte for inhibiting pepsin and treating microbial infections. *Saudi J Biol Sci,* **28**(11), 6245–6253. doi: 10.1016/j.sjbs.2021.06.090.

Sha'bani N., Miraj S., Rafieian-Kohpayei M. and Namjoo A.R. (2015). Survey of the detoxification effect of green tea extract on the reproductive system in rats exposed to lead acetate. *Adv Biomed Res,* **4**, 155.

Shaheen I. and Ahmad K.S. (2022). Biomimetic Synthesis of Highly Reusable MoO3-based Catalysts for Fast Degradation of Azo Dyes. *Materials Innovations* **9**.10, 255–268.

Sığırcık G., Tüken T. and Erbil M. (2016). Assessment of the inhibition efficiency of 3,4-diaminobenzonitrile against the corrosion of steel. *Corrosion Science,* **102**, 437-445. doi: https://doi.org/10.1016/j.corsci.2015.10.036.

Wedian F., Al-Qudah M.A. and Al-Mazaideh G.M. (2017). Corrosion Inhibition of Copper by Capparis spinosa L. Extract

in Strong Acidic Medium: Experimental and Density Functional Theory. *International Journal of Electrochemical Science,* **12**, 4664–4676. doi: 10.20964/2017.06.47.

Wedian F., Mhaidat I., Braik N.A. and Al-Mazaideh G.M. (2022). A corrosion inhibitor for aluminum by novel synthesized triazole compounds in basic medium. *International Journal of Corrosion and Scale Inhibition,* **11**(1), 364–381. doi: 10.17675/2305-6894-2022-11-1-22.

Wedian F., Mhaidat I., Braik N.A. and Al-Mazaideh G.M. (2022). A corrosion inhibitor for aluminum by novel synthesized triazole compounds in basic medium. **11**(1), 364–381.

Wedian F., Mifrig A.Z. and Al-Mazaideh G.M. (2022). Inhibition impact of synthesized mercapto- and alkylthio-triazole compounds on the corrosion of aluminum in acidic solution. *International Journal of Corrosion and Scale Inhibition,* **11**(3), 1083–1099.